Influence of MHD and heat/mass transfer on the peristaltic flow of Johnson Segalman fluid in a curved channel with permeable compliant walls

Ali M. Kamal[1] , Ahmed M. Abdulhadi[2]

College of science,University of Baghdad, Baghdad- Iraq.

E-mail[1]: alikammal82@gmail.com , E-mail[2]: ahm6161@yahoo.com

Abstract

Analysis has been made for the curvature effects on the MHD and heat transfer peristaltic flow of an incompressible Johnson-Segalman fluid in a channel. The flow problem is first reduced in the wave frame of reference and then solved after employing the long wavelength and low Reynolds number approximations. Expressions for stream function, magnetic force function, temperature and concentration fields are derived. The effects of emerging parameters in the obtained solutions are plotted and analyzed.

Keywords: Curved channel, Induced magnetic field, Heat transfer, Permeable wall.

1. Intoduction

The peristaltic transport phenomena have immense theoretical and technical applications in physiology and industry, for example in biomedical engineering, pumping of blood in dialysis and in industries, and transport of toxic liquid in nuclear industry. It also occurs in the transport of urine from kidney to bladder, chyme motion in the gastrointestinal tract, blood transport in capillaries, intra-uterine fluid motion, movement of ovum in the female fallopian tube, etc. Latham [1] and Jaffrin and Shapiro [2] initially discussed the process of peristalsis in tube/channel. Keeping in mind the importance of processes of hemodialysis and oxygenation, several researches were conducted on the study of heat transfer in peristalsis. Radhakrishnamacharya and Murty[3] investigated the characteristics of heat transfer in the peristaltic flow through a non-uniform channel. Vajravelu et al.[4] considered the peristaltic flow in an annulus by using the approximation of long wavelength. Srinivas and Kothandapani [5] examined the heat transfer in peristaltic flow in an asymmetric channel. Heat transfer characteristics in the hydromagnetic flow with peristalsis were explored by Mekheimer and Elmaboud [6]. Srinivas et al.[7] studied the features of convective heat and mass transfer in the peristaltic transport through an asymmetric channel. Influence of chemical reaction and space porosity on the hydromagnetic peristaltic transport in an asymmetric channel was reported by Srinivas and Muthraj [8]. Nadeem and Akbar [9] considered the magnetohydrodynamics (MHD) peristaltic motion with heat and mass transfer. Induced magnetic field influences on peristalsis were described by Elmaboud [10]. Tripathi et al.[11] analyzed the peristaltic motion in gerenalized Burgers' fluid. Further, Tripathi [12] examined the peristaltic transport of chyme movement in small intestine.

There is a subclass of differential type fluids known as Johnson-Segalman fluid. This fluid model is one subclass of non-Newtonian fluids which can explain the ''spurt'' phenomenon. The term ''spurt'' Has been used for the description of large increase in the volume to a small increase in the driving pressure gradient. Hayat et al. [13] examined the peristaltic flow of Johnson-Segalman fluid in a planar channel. Elshahed and Haroun [14] studied the peristaltic motion of Johnson-Segalman fluid under the effect of magnetic field. The peristaltic transport of Johnson-Segalman fluid in an asymmetric channel has been discussed by Hayat et al. [15]. Wang et al. [16] studied the peristaltic motion of Johnson–Segalman fluid through a deformable tube. Nadeem and Akbar [17] studied the

effects of induced magnetic field and heat and mass transfer on peristaltic flow of Johnson-Segalman fluid in a vertical asymmetric channel.

Peristaltic transport in curved channel is another important area of research which is not yet given a due attention. All the above mentioned studies have been undertaken in straight channels/tubes. Flow over curved channels is relevant to many industrial, biological and environmental applications. Examples are the spreading of pollution in a fjord and the wear experienced by pipes going through rough oceanic terrain. It is known that shape of most of the physiological tubes and glandular ducts is curved. Laser guiding in curved plasma channels have important applications such as an efficient circular x-ray laser medium, optical synchrotrons, laser accelerators and harmonic generators. Flow characteristics during flood associated with sediments transport is an application of curved geometry from engineering point of view. Micro heat exchangers involve curved channels where goal is often to increase the heat flux while limiting the pressure drop. Ali et al. [18] discussed the peristaltic flow of viscous fluid in a curved channel. Later on, they [19] extended the analysis by considering the heat transfer characteristics. Very recently Ali et al. [20] studied the peristaltic motion of third grade fluid in a curved channel.

The main purpose of this current investigation is to discuss the induced magnetic field, heat transfer, mass transfer and permeable walls effects on the peristaltic flow of J-S fluid in acurvedchannel. Hence the Johnson-Segalman fluid in a curved channel with flexible permeable walls is considered. The relevant equations are modeled first time. Series solutions are developed for small Weissenberg number. Graphs for the interesting quantities are plotted and interpreted.

2. Mathematical modeling

Consider the flow of an incompressible J-S fluid in a curved channel of radius R^* and uniform thickness $2d_1$ coiled in a circle with centre o (see Fig. 1). We denote axial and radial directions by x and r. Here u and v are the components of velocity in the axial and radial directions respectively.The wave shapes are

$$r = \pm\eta(x,t) = \pm\left[d_1 + a\sin\frac{2\pi}{\lambda}(x - ct) \right], \tag{1}$$

Where c is the wave speed and a and λ are the wave amplitude and wavelength respectively.

The equations which can govern the flow are:

$$\frac{\partial v}{\partial r} + \frac{R^*}{r+R^*}\frac{\partial u}{\partial x} + \frac{v}{r+R^*} = 0. \tag{2}$$

$$\rho\left[\frac{\partial v}{\partial t} + v\frac{\partial v}{\partial r} + \frac{R^*\mathrm{u}}{r+R^*}\frac{\partial v}{\partial x} - \frac{\mathrm{u}^2}{r+R^*} \right] = -\frac{\partial p}{\partial r} + \frac{1}{r+R^*}\frac{\partial}{\partial r}\left\{ (r+R^*)\tau_{rr} \right\} + \frac{R^*}{r+R^*}\frac{\partial \tau_{xr}}{\partial x} - \frac{\tau_{xx}}{r+R^*} - \frac{\eta_1}{\alpha}v\,, \tag{3}$$

$$\rho\left[\frac{\partial u}{\partial t} + v\frac{\partial u}{\partial r} + \frac{R^*\mathrm{u}}{r+R^*}\frac{\partial u}{\partial x} + \frac{\mathrm{u}v}{r+R^*} \right] = -\frac{R^*}{r+R^*}\frac{\partial p}{\partial x} + \frac{1}{(r+R^*)^2}\frac{\partial}{\partial r}\left\{ (r+R^*)^2\tau_{rx} \right\} + \frac{R^*}{r+R^*}\frac{\partial \tau_{xx}}{\partial x} - \left(\frac{\eta_1}{\alpha} + \sigma B_0^2 \right)u. \tag{4}$$

The energy equation becomes

$$\rho C_p\left[\frac{\partial}{\partial t} + v\frac{\partial}{\partial r} + \frac{R^*\mathrm{u}}{r+R^*}\frac{\partial}{\partial x} \right]T = \kappa\left[\frac{\partial^2}{\partial r^2} + \frac{1}{r+R^*}\frac{\partial}{\partial r} + \frac{\partial^2}{\partial x^2} \right]T$$

$$+(S_{rr} - S_{xx})\frac{\partial v}{\partial r} + S_{xr}\left(\frac{\partial u}{\partial r} + \frac{R^*}{r+R^*}\frac{\partial v}{\partial x} - \frac{u}{r+R^*} \right) \tag{5}$$

and concentration field satisfies

$$\left[\frac{\partial}{\partial t}+v\frac{\partial}{\partial r}+\frac{R^{*}\mathrm{u}}{r+R^{*}}\frac{\partial}{\partial x}\right]C=D\left[\frac{\partial^{2}}{\partial r^{2}}+\frac{1}{r+R^{*}}\frac{\partial}{\partial r}+\frac{\partial^{2}}{\partial x^{2}}\right]C+\frac{DK_{T}}{T_{m}}\left[\frac{\partial^{2}}{\partial r^{2}}+\frac{1}{r+R^{*}}\frac{\partial}{\partial r}+\frac{\partial^{2}}{\partial x^{2}}\right]T. \tag{6}$$

The Cauchy stress tensor $\boldsymbol{\tau}$ in a Johnson-Segalman fluid is :

$$\boldsymbol{\tau}=2\mu\mathbf{D}+\mathbf{S},$$

$$\mathbf{S}+m\left[\frac{d\mathbf{S}}{dt}+\mathbf{S}(\mathbf{W}-\xi\mathbf{D})+(\mathbf{W}-\xi\mathbf{D})^{T}\mathbf{S}\right]=2\eta_{1}\mathbf{D},$$

Where the symmetric (**D**) and skew symmetric (**W**) parts of velocity gradient are

$$\mathbf{D}=\frac{1}{2}\left[\nabla\mathbf{V}+(\nabla\mathbf{V})^{T}\right],\quad \mathbf{W}=\frac{1}{2}\left[\nabla\mathbf{V}-(\nabla\mathbf{V})^{T}\right].$$

The above relations yield

$$S_{rr}+m\left[\frac{dS_{rr}}{dt}-\frac{2\,\mathrm{u}\,S_{rx}}{r+R^{*}}+S_{rx}\left\{(1-\xi)\frac{\partial u}{\partial r}-\frac{1+\xi}{r+R^{*}}\left[R^{*}\frac{\partial v}{\partial x}-u\right]\right\}-2\xi S_{rr}\frac{\partial v}{\partial r}\right]=2\eta_{1}\frac{\partial v}{\partial r}\ , \tag{7}$$

$$\eta_{1}\left(\frac{\partial u}{\partial r}+\frac{R^{*}}{r+R^{*}}\frac{\partial v}{\partial x}-\frac{u}{r+R^{*}}\right)=S_{rx}+m\frac{dS_{rx}}{dt}+\frac{mu(S_{rr}-S_{xx})}{r+R^{*}}+\frac{mS_{xx}}{dt}\left\{(1-\xi)\frac{\partial u}{\partial r}-\frac{1+\xi}{r+R^{*}}\left[R^{*}\frac{\partial v}{\partial x}-u\right]\right\}$$
$$+m\frac{S_{rr}}{2}\left\{\frac{(1-\xi)}{r+R^{*}}\left[R^{*}\frac{\partial v}{\partial x}-u\right]-(1+\xi)\frac{\partial u}{\partial r}\right\}, \tag{8}$$

$$S_{xx}+m\left[\frac{dS_{xx}}{dt}-\frac{2\,\mathrm{u}\,S_{rx}}{r+R^{*}}-S_{rx}\left\{(1+\xi)\frac{\partial u}{\partial r}-\frac{1-\xi}{r+R^{*}}\left[R^{*}\frac{\partial v}{\partial x}-u\right]\right\}+2\xi S_{xx}\frac{\partial v}{\partial r}\right]=-2\eta_{1}\frac{\partial v}{\partial r}\ , \tag{9}$$

Where $d/dt=\partial/\partial t+v\partial/\partial r+uR^{*}/(r+R^{*})\partial/\partial x$ is the material time derivative, P the pressure, μ and η_{1} are the viscosities, m the relaxation time, ρ the density, R^{*} the curvature parameter, τ_{1} the elastic tension, m_{1} the mass per unit area, d the coefficient of viscous damping, **D** and **W** are the symmetric and skew symmetric parts of velocity gradient, ξ is the slip parameter and S_{xr}, S_{rr} and S_{xx} and the components of an extra stress tensor **S**.

The boundary conditions can be written as

$$u=0,\ T=T_{0},\ C=C_{0}\ \text{ at }\ r=\pm\eta, \tag{10}$$

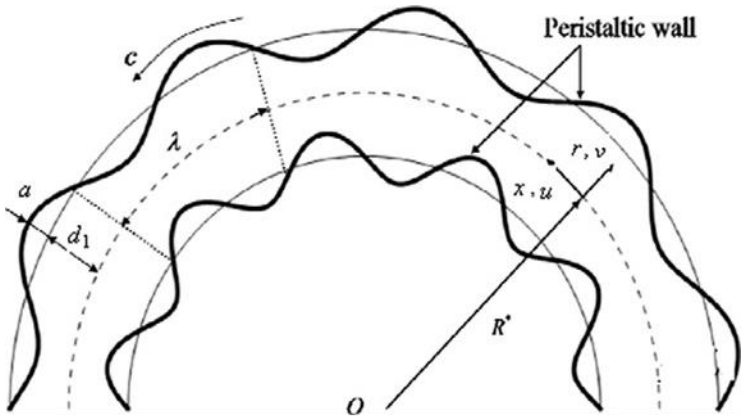

Fig. 1. Physical model

$$R^*\left[-\tau_1\frac{\partial^3}{\partial x^3}+m_1\frac{\partial^3}{\partial x\partial t^2}+d\frac{\partial^2}{\partial t\partial x}\right]\eta=\frac{1}{(r+R^*)}\frac{\partial}{\partial r}\left\{(r+R^*)^2\tau_{rx}\right\}+R^*\frac{\partial\tau_{xx}}{\partial x}$$

$$-\rho(r+R^*)\left[\frac{\partial u}{\partial t}+v\frac{\partial u}{\partial r}+\frac{R^*\mathrm{u}}{r+R^*}\frac{\partial u}{\partial x}+\frac{\mathrm{u}v}{r+R^*}\right]\ \text{at}\ r=\pm\eta. \tag{11}$$

Definig

$$u^*=\frac{u}{c},\ v^*=\frac{v}{c},\ r^*=\frac{r}{d_1},\ t^*=\frac{ct}{\lambda},\ \eta^*=\frac{\eta}{d_1},\ k=\frac{R^*}{d_1},\ W_e=\frac{mc}{d_1},D_a=\frac{\alpha}{d_1^2},\ M^2=\frac{\sigma B_0^2 d_1^2}{\eta_1},$$

$$p^*=\frac{d_1^2 p}{c\lambda(\mu+\eta_1)},\quad S_{ij}^*=\frac{d_1 S_{ij}}{c\eta_1},\ \theta=\frac{T-T_0}{T_0},\ \phi=\frac{C-C_0}{C_0},\psi^*=\frac{\psi}{cd_1},\ x^*=\frac{x}{\lambda},$$

Eqs. (3)-(10) and (11) become

$$2\frac{\partial v}{\partial r}=S_{rr}+W_e\left[\left(\delta\frac{\partial}{\partial t}+v\frac{\partial}{\partial r}+\frac{uk\delta}{r+k}\frac{\partial}{\partial x}\right)S_{rr}-\frac{2uS_{rx}}{r+k}-2\xi S_{rr}\frac{\partial v}{\partial r}\right]$$
$$+W_eS_{rx}\left\{(1-\xi)\frac{\partial u}{\partial r}-\frac{1+\xi}{r+k}\left(k\delta\frac{\partial v}{\partial x}-u\right)\right\}, \tag{12}$$

$$\left(\frac{\partial u}{\partial r}+\frac{k\delta}{r+k}\frac{\partial v}{\partial x}-\frac{u}{r+k}\right)=S_{rx}+W_e\left[\left(\delta\frac{\partial}{\partial t}+v\frac{\partial}{\partial r}+\frac{uk\delta}{r+k}\frac{\partial}{\partial x}\right)S_{rx}+\frac{u(S_{rr}-S_{xx})}{r+k}\right]$$
$$+\frac{W_eS_{rr}}{2}\left\{\frac{1-\xi}{r+k}\left(k\delta\frac{\partial v}{\partial x}-u\right)-(1+\xi)\frac{\partial u}{\partial r}\right\}+\frac{W_eS_{xx}}{2}\left\{(1-\xi)\frac{\partial u}{\partial r}-\frac{1+\xi}{r+k}\left[k\delta\frac{\partial v}{\partial x}-u\right]\right\}, \tag{13}$$

$$-2\frac{\partial v}{\partial r}=S_{xx}+W_e\left[\left(\delta\frac{\partial}{\partial t}+v\frac{\partial}{\partial r}+\frac{uk\delta}{r+k}\frac{\partial}{\partial x}\right)S_{xx}-\frac{2uS_{rx}}{r+k}-2\xi S_{xx}\frac{\partial v}{\partial r}\right]$$
$$+\left\{\frac{1-\xi}{r+k}\left(k\delta\frac{\partial v}{\partial x}-u\right)-(1+\xi)\frac{\partial u}{\partial r}\right\} \tag{14}$$

$$R_e\delta\left[\delta\frac{\partial v}{\partial t}+v\frac{\partial v}{\partial r}+\frac{uk\delta}{r+k}\frac{\partial v}{\partial x}-\frac{u^2}{r+k}\right]=-\frac{\eta_1+\mu}{\eta_1}\frac{\partial p}{\partial r}+\frac{4\delta\mu}{\eta_1(r+k)}\frac{\partial v}{\partial r}+\frac{k\delta^2}{r+k}+\delta\frac{\partial S_{rx}}{\partial x}+\delta\frac{\partial S_{rr}}{\partial r}$$
$$+\frac{\delta(S_{rr}-S_{xx})}{r+k}+\frac{\delta\mu}{\eta_1}\frac{\partial^2 v}{\partial r^2}+\frac{\delta^2k\mu}{\eta_1(r+k)}\frac{\partial}{\partial x}\left(\frac{\partial u}{\partial r}+\frac{k\delta}{r+k}\frac{\partial v}{\partial x}-\frac{u}{r+k}\right)-\frac{\delta}{D_a}v, \tag{15}$$

$$R_e\delta\left[\delta\frac{\partial u}{\partial t}+v\frac{\partial u}{\partial r}+\frac{uk\delta}{r+k}\frac{\partial u}{\partial x}-\frac{uv}{r+k}\right]=-\frac{(\eta_1+\mu)k}{\eta_1(r+k)}\frac{\partial p}{\partial x}+\frac{\partial S_{rx}}{\partial r}+\frac{2S_{rx}}{r+k}+\frac{k\delta}{r+k}\frac{\partial S_{xx}}{\partial x}-\frac{2\delta k\mu}{\eta_1(r+k)}$$
$$\times\frac{\partial^2 v}{\partial r\partial x}+\frac{\mu}{\eta_1}\frac{\partial}{\partial r}\left(\frac{\partial u}{\partial r}+\frac{k\delta}{r+k}\frac{\partial v}{\partial x}-\frac{u}{r+k}\right)-\left(\frac{1}{D_a}+M^2\right)u, \tag{16}$$

$$R_e\left[\delta\frac{\partial}{\partial t}+v\frac{\partial}{\partial r}+\frac{uk\delta}{r+k}\frac{\partial}{\partial x}\right]\theta=E\left[(S_{rr}-S_{xx})\frac{\partial v}{\partial r}+S_{xr}\left(\frac{\partial u}{\partial r}+\frac{k\delta}{r+k}\frac{\partial v}{\partial x}-\frac{u}{r+k}\right)\right]$$
$$+\frac{1}{p_r}\left[\frac{\partial^2}{\partial r^2}+\frac{1}{r+k}\frac{\partial}{\partial r}+\delta^2\frac{\partial^2}{\partial x^2}\right]\theta, \tag{17}$$

$$R_e\left[\delta\frac{\partial}{\partial t}+v\frac{\partial}{\partial r}+\frac{uk\delta}{r+k}\frac{\partial}{\partial x}\right]\phi=\frac{1}{S_c}\left[\frac{\partial^2}{\partial r^2}+\frac{1}{r+k}\frac{\partial}{\partial r}+\delta^2\frac{\partial^2}{\partial x^2}\right]\phi+S_r\left[\frac{\partial^2}{\partial r^2}+\frac{1}{r+k}\frac{\partial}{\partial r}+\delta^2\frac{\partial^2}{\partial x^2}\right]\theta, \quad (18)$$

With the boundary conditions

$$u=0,\ \theta=0,\ \phi=0 \quad \text{at } r=\pm\eta=\pm(1+\epsilon\sin 2\pi(x-t)), \quad (19)$$

$$k\left[E_1\frac{\partial^3}{\partial x^3}+E_2\frac{\partial^3}{\partial x\partial t^2}+E_3\frac{\partial^2}{\partial t\partial x}\right]\eta=\frac{\eta_1(r+k)}{(\eta_1+\mu)}\left[\frac{\partial}{\partial r}\left(\frac{\partial u}{\partial r}+\frac{k\delta}{r+k}\frac{\partial v}{\partial x}-\frac{u}{r+k}\right)-\frac{2k\delta}{r+k}\frac{\partial^2 v}{\partial r\partial x}\right]$$
$$-\frac{R_e\mu(r+k)}{(\eta_1+\mu)}\left[\delta\frac{\partial u}{\partial t}+v\frac{\partial u}{\partial r}+\frac{uk\delta}{r+k}\frac{\partial u}{\partial x}+\frac{uv}{r+k}\right]+\frac{\eta_1(r+k)}{(\eta_1+\mu)}\left[\frac{\partial S_{rx}}{\partial r}+\frac{2S_{rx}}{r+k}+\frac{k\delta}{r+k}\frac{\partial S_{xx}}{\partial x}\right]$$
$$+\frac{2\mu}{(\eta_1+\mu)}\left(\frac{\partial u}{\partial r}+\frac{k\delta}{r+k}\frac{\partial v}{\partial x}-\frac{u}{r+k}\right) \quad \text{at } (r=\pm\eta). \quad (20)$$

Note that the continuity Eq. (2) is satisfied identically, $\epsilon(=a/d_1)$ isthe amplitude ratio, $\delta(=d_1/\lambda)$ the wave number, k the dimensionless curvature parameter, R_e $(=c\rho d_1/\eta_1)$ the Reynolds number, $W_e(=mc/d_1)$ the Weissenberg number, $D_a(=\alpha/d_1^2)$ the Darcy number, M $(=\sqrt{\sigma/\eta_1}B_0d_1)$ the Hartman number, P_r $(=\mu C_p/\kappa)$ the Prandtl number, E $(=c^2/C_pT_0)$ the Eckert number, S_c $(=\mu/\rho d)$ the Schmidt number, S_r $(=\rho T_0DK_T/\mu T_mC_0)$ the Soret number, $B_r(=EP_r)$ the Brinkman number and $E_1(=-\tau_1d_1^3/\lambda^3\eta_1c)$, $E_2(=m_1cd_1^3/\lambda^3\eta_1)$, $E_3(=dd_1^3/\lambda^2\eta_1)$ represents the non-dimensional elasticity parameters. In particular, rigid nature of the wall is explained by the parameter E_1, which depends upon the wall tension, E_2 gives the stiffness property of the wall and E_3 describes the dissipative feature of the wall. For $E_3 = 0$, the wall moves up and down with no damping force on it. This situation corresponds to the case of elastic walls. If $\psi(x,y,t)$ is the stream function then writing

$$u=-\frac{\partial\psi}{\partial r}, \quad v=\delta\frac{k}{k+r}\frac{\partial\psi}{\partial x},$$

expressions (12)-(20) after using long wavelength and low Reynold's number give

$$\frac{\partial p}{\partial r}=0, \quad (21)$$

$$-\frac{k(\eta_1+\mu)}{\eta_1(r+k)}\frac{\partial p}{\partial x}+\frac{\partial S_{rx}}{\partial r}+\frac{2S_{rx}}{r+k}+\frac{\mu}{\eta_1}\frac{\partial}{\partial r}\left(-\psi_{rr}+\frac{\psi_r}{r+k}\right)$$
$$+\frac{2\mu}{(r+k)\eta_1}\left(-\psi_{rr}+\frac{\psi_r}{r+k}\right)-\left(\frac{1}{D_a}+M^2\right)\psi_r=0, \quad (22)$$

$$\left[\frac{\partial^2}{\partial r^2}+\frac{1}{r+k}\frac{\partial}{\partial r}\right]\theta=-B_r\left[S_{xr}\left(-\psi_{rr}+\frac{\psi_r}{r+k}\right)\right], \quad (23)$$

$$\left[\frac{\partial^2}{\partial r^2}+\frac{1}{r+k}\frac{\partial}{\partial r}\right]\phi=-S_cS_r\left[\frac{\partial^2}{\partial r^2}+\frac{1}{r+k}\frac{\partial}{\partial r}\right]\theta, \quad (24)$$

$$\psi_r=0,\ \theta=0,\ \phi=0 \ \text{ at } r=\pm\eta=\pm(1+\epsilon\sin 2\pi(x-t)), \quad (25)$$

$$k\left[E_1\frac{\partial^3}{\partial x^3}+E_2\frac{\partial^3}{\partial x\partial t^2}+E_3\frac{\partial^2}{\partial t\partial x}\right]\eta=\frac{\eta_1(r+k)}{(\eta_1+\mu)}\left[\frac{\mu}{\eta_1}\frac{\partial}{\partial r}\left(-\psi_{rr}+\frac{\psi_r}{r+k}\right)+\frac{\partial S_{rx}}{\partial r}+\frac{2S_{rx}}{r+k}\right]$$
$$+\frac{2\mu}{(\eta_1+\mu)}\left(-\psi_{rr}+\frac{\psi_r}{r+k}\right) \quad \text{at } (r=\pm\eta), \quad (26)$$

With

$$0 = S_{rr} + W_e S_{rx}\left[-(1-\xi)\psi_{rr} - \frac{1+\xi}{r+k}\psi_r + \frac{2\psi_r}{r+k}\right], \tag{27}$$

$$\left(-\psi_{rr} + \frac{\psi_r}{r+k}\right) = -W_e\frac{\psi_r(S_{rr}-S_{xx})}{r+k} + \frac{W_e S_{rr}}{2}\left\{\frac{1-\xi}{r+k}\psi_r + (1+\xi)\psi_{rr}\right\}$$

$$+ S_{rx} - \frac{W_e S_{xx}}{2}\left\{(1-\xi)\psi_{rr} + \frac{1+\xi}{r+k}\psi_r\right\}, \tag{28}$$

$$0 = S_{xx} + W_e S_{rx}\left[-\frac{2\psi_r}{r+k} + \left\{\frac{1-\xi}{r+k}\psi_r + (1+\xi)\psi_{rr}\right\}\right]. \tag{29}$$

From Eqs. (27)-(29) one has

$$S_{rx} = \left(-\psi_{rr} + \frac{\psi_r}{r+k}\right)\left[1 + W_e^2(1-\xi^2)\left(-\psi_{rr} + \frac{\psi_r}{r+k}\right)^2\right]^{-1}. \tag{30}$$

Due to Eqs. (21) and (22) one obtains

$$(k+r)\frac{\partial^2 S_{rx}}{\partial r^2} + 3\frac{\partial S_{rx}}{\partial r} + \frac{(k+r)\mu}{\eta_1}\frac{\partial^2}{\partial r^2}\left(-\psi_{rr} + \frac{\psi_r}{r+k}\right) + \frac{3\mu}{\eta_1}\frac{\partial}{\partial r}\left(-\psi_{rr} + \frac{\psi_r}{r+k}\right)$$

$$+(r+k)\left(\frac{1}{D_a} + M^2\right)\left(-\psi_{rr} + \frac{\psi_r}{r+k}\right) = 0. \tag{31}$$

2. Solution procedure

Different from the work reported in [21], in which the authors have obtained the exact solutions, here the differential system is strongly non-linear and cannot be solved exactly. We therefore first proceed for the perturbation solution and write streame function, stress components, temperature distribution, concentration field and heat transfer coefficient as:

$$\psi = \psi_0 + W_e^2\psi_1 + ..., \tag{32}$$

$$S_{rx} = S_{0rx} + W_e^2 S_{1rx} + ..., \tag{33}$$

$$S_{rr} = S_{0rr} + W_e^2 S_{1rr} + ..., \tag{34}$$

$$S_{xx} = S_{0xx} + W_e^2 S_{1xx} + ..., \tag{35}$$

$$\theta = \theta_0 + W_e^2\theta_1..., \tag{36}$$

$$\phi = \phi_0 + W_e^2\phi_1..., \tag{37}$$

$$Z = Z_0 + W_e^2 Z_1..., \tag{38}$$

3.1. *Zeroth order system*

Putting Eqs. (32)-(37) into Eqs. (23)-(26), (30) and (31) and then equating the coefficients of W_{e^0} we arrive at

$$(k+r)\frac{\partial^2}{\partial r^2}\left(-\psi_{0rr} + \frac{\psi_{0r}}{r+k}\right) + 3\left(-\psi_{0rr} + \frac{\psi_{0r}}{r+k}\right) + A_1(k+r)\left(-\psi_{0rr} + \frac{\psi_{0r}}{r+k}\right) = 0, \tag{39}$$

$$\left[\frac{\partial^2}{\partial r^2} + \frac{1}{r+k}\frac{\partial}{\partial r}\right]\theta_0 = -B_r\left[S_{0xr}\left(-\psi_{0rr} + \frac{\psi_{0r}}{r+k}\right)\right], \tag{40}$$

$$\left[\frac{\partial^2}{\partial r^2} + \frac{1}{r+k}\frac{\partial}{\partial r}\right]\phi_0 = -S_c S_r\left[\frac{\partial^2}{\partial r^2} + \frac{1}{r+k}\frac{\partial}{\partial r}\right]\theta_0, \tag{41}$$

$$\psi_{0r} = 0,\ \theta_0 = 0,\ \phi_0 = 0 \quad \text{at } (r = \pm\eta), \tag{42}$$

$$k\left[E_1\frac{\partial^3}{\partial x^3} + E_2\frac{\partial^3}{\partial x\partial t^2} + E_3\frac{\partial^2}{\partial t\partial x}\right]\eta = (k+r)\frac{\partial}{\partial r}\left(-\psi_{0rr} + \frac{\psi_{0r}}{r+k}\right) + 2\left(-\psi_{0rr} + \frac{\psi_{0r}}{r+k}\right) \text{ at } (r = \pm\eta), \tag{43}$$

Where

$$S_{0xr} = \left(-\psi_{0rr} + \frac{\psi_{0r}}{r+k}\right).$$

The solution of above equations are

$$\psi_0 = c_4 + \frac{(k+r)(\pi(k+r)(4c_3 + A_1^{1/2}(1-2\ln(k+r)c_1)l_1 + 8c_2 l_2 l_1^2))}{8\pi l_1}, \tag{44}$$

and at this order

$$u_0 = -\psi_{0r} = \frac{1}{2}(k+r)(A^{1/2}\ln(k+r)c_1 - 2c_3) + \frac{c_2(1-2(1+\gamma+l_2)l_1^2}{\pi l_1}, \tag{45}$$

$$\theta_0 = c_6 + c_5\ln(k+r) + \frac{1}{48\pi^2 l_1^2}B_r(3A_1\pi^2(r(2k+r) - 2k^2\ln(k+r)c_1^2 l_1^2 + 48A^{1/2}\pi c_1 c_2 l_1$$
$$\times(-r + k\ln(k+r) + (2r(-2+\gamma+l_2 + k\ln(k+r)(4-2\gamma+\ln(4)+2\ln(k+r) - 2\ln(A^{1/2}(k+r)))l_1^2$$
$$+8\ln(k+r)c_2^2(3\ln(k+r) - 4(3l_2^2 + \ln(k+r)(3\gamma+\ln(8)+\ln(k+r) - 3\ln(A^{1/2}(k+r)))l_1^2$$
$$+2(\ln(k+r)(6\gamma^2 + 4\gamma\ln\left(\frac{(k+r)^2}{(k+r)}\right) + 4\ln(k+r)(-3\gamma+\ln(k+r)l_2$$
$$-6(-2\gamma+\ln(k+r))l_2 + 4l_2 l_1)), \tag{46}$$

$$\phi_0 = -S_c S_r\theta_0, \tag{47}$$

$$Z_0 = \eta_x\theta_{0r}(\eta), \tag{48}$$

$$A_1 = \frac{\eta_1(1+D_a M^2)}{(\eta_1+\mu)D_a}, \quad l_1 = \frac{A_1^{1/2}(k+r)}{2}, \quad l_2 = \ln\left(\frac{1}{2}A_1^{1/2}(k+r)\right).$$

3.2. *First order system*

The coefficients of $O(W_e^0)$ leads to the following expressions

$$0 = (k+r)\frac{\partial^2}{\partial r^2}\left[\left(-\psi_{1rr} + \frac{\psi_{1r}}{r+k}\right) - A_2\left(-\psi_{1rr} + \frac{\psi_{1r}}{r+k}\right)^3\right]$$
$$+3\frac{\partial}{\partial r}\left[\left(-\psi_{1rr} + \frac{\psi_{1r}}{r+k}\right) - A_2\left(-\psi_{1rr} + \frac{\psi_{1r}}{r+k}\right)^3\right] + A_3(k+r)\left(-\psi_{1rr} + \frac{\psi_{1r}}{r+k}\right), \tag{49}$$

$$\left[\frac{\partial^2}{\partial r^2} + \frac{1}{r+k}\frac{\partial}{\partial r}\right]\theta_1 = -B_r\left[S_{1xr}\left(-\psi_{0rr} + \frac{\psi_{0r}}{r+k}\right) + S_{0xr}\left(-\psi_{1rr} + \frac{\psi_{1r}}{r+k}\right)\right], \tag{50}$$

$$\left[\frac{\partial^2}{\partial r^2} + \frac{1}{r+k}\frac{\partial}{\partial r}\right]\phi_1 = -S_c S_r\left[\frac{\partial^2}{\partial r^2} + \frac{1}{r+k}\frac{\partial}{\partial r}\right]\theta_1, \tag{51}$$

$$\psi_{1r} = 0,\ \theta_1 = 0,\ \phi_1 = 0 \quad \text{at } (r = \pm\eta), \tag{52}$$

$$0=(k+r)\frac{\partial}{\partial r}\left[\left(-\psi_{1rr}+\frac{\psi_{1r}}{r+k}\right)-A_2\left(-\psi_{1rr}+\frac{\psi_{1r}}{r+k}\right)^3\right]$$

$$+2\left[\left(-\psi_{1rr}+\frac{\psi_{1r}}{r+k}\right)-A_2\left(-\psi_{1rr}+\frac{\psi_{1r}}{r+k}\right)^3\right] \text{ at } (r=\pm\eta), \tag{53}$$

$$S_{1rx}=\left(-\psi_{1rr}+\frac{\psi_{1r}}{r+k}\right)-(1-\xi^2)\left(-\psi_{1rr}+\frac{\psi_{1r}}{r+k}\right)^3. \tag{54}$$

Putting the zeroth order solution expressions into first order system and then solving the resulting problems we have

$$\psi_1=c_{10}+\frac{1}{864\pi^3(k+r)l_1^3}(-648A_1A_2\pi^2(k+r)^2c_1^2c_2l_1^2(-1+2(\gamma+l_2l_1^2-216A_1A_2\pi(k+r)c_1c_2^2l_1$$
$$\times(3\ln(k+r)-6((1+2\gamma)\ln(k+r)+l_2^2+2((3+6\gamma+6\gamma^2)\ln(k+r)+l_2^2(3+6\gamma+2l_2)l_1^4)$$
$$+32A_2c_2^3(-9+18(4+3\gamma+3l_2l_1^2-12(26+24\gamma+9\gamma^2+6(4+3\gamma)l_2+9l_2l_1^4$$
$$+8(80+78\gamma+36\gamma^2+9\gamma^3+(26+24\gamma+9\gamma^3+3(26+24\gamma+9\gamma^2)l_2+9(4+3\gamma)l^2+9l_2^3l_1^6$$
$$+27\pi^2(k+r)^2l_1^2(\pi(k+r)(16c_9+4A_1^{1/2}(1-2\ln(k+r))c_7+A_1^{3/2}A_2(-1+2\ln(k+r)c_1^3)l_1$$
$$+32c_8(-1+2(\gamma+l_2l_1^2))), \tag{55}$$

$$u_1=-\psi_{1r}=\frac{1}{216\pi^3(k+r)^2l_1^3}(162A_1A_2\pi^2(k+r)^2c_1^2c_2l_1^2(-1+2(1+\gamma+l_2l_1^2)$$
$$+162A_1^{1/2}A_2\pi(k+r)c_1c_2^2l_1(1-2(1+2\gamma+2l_2)l_1^2+(2+4\gamma+4\gamma^2+(4+8\gamma)l_2+4l_2^2)l_1^4$$
$$+8A_2c_2^3(-9+18(1+3\gamma+3l_2)l_1^2-12(2+6\gamma+9\gamma^2+6(1+3\gamma)l_2+4l_2^2l_1^4$$
$$+9(1+3\gamma)\ln(\frac{1}{2}A_1^{1/2}(k+r))^2+9\ln(\frac{1}{2}A_1^{1/2}(k+r))^3)l_1^6+8c_8(-1+2(1+\gamma+l_2)l_1^2))), \tag{56}$$

$$\theta_1=c_{12}+\frac{1}{16}(\frac{1}{4}A_1B_r(k+r)^2c_1(-8c_7+A_1(1+2A_2-\xi^2)c_1^3)+\frac{1}{\pi l_1}8A_1^{1/2}B_r(k+r)$$
$$(-2c_8c_1+(-2c_7+A_1(1+2A_2-\xi^2)c_1^3)c_2)(-1+2(-2+\gamma)l_1^2+8(24+18\gamma+6\gamma^2+\gamma^3)l_1^6)$$
$$+\frac{1}{\pi^2l_1^2}8\ln(k+r)(2\pi^2c_{11}l_1^2-B_r\left(\ln\frac{\frac{1}{2}A^{1/2}(k+r)}{(k+r)}\right)c_1^2c_2^2(1-2\gamma l_1^2)^2+l_3c_2l_1^2(-4\pi^2(k+r)^2c_8$$
$$+3(1+2A_2-\xi^2)c_2(A_1\pi^2(k+r)^2c_1^2+8c_2^2l_1^2+6l_3(-2A_1^{1/2}\pi^3(k+r)^3c_8c_1l_1^3-A^{1/2}\pi^3(k+r)^3$$
$$+\frac{2}{3}l_3^3c_2(-4\pi^2(k+r)^2c_8+\frac{1}{6}l_3^2c_2(-4\pi^2(k+r)^2c_8(6+8\gamma+4\gamma^2)l_1^4)), \tag{57}$$

$$\phi_1=-S_cS_r\theta_1, \tag{58}$$
$$Z_1=\eta_x\theta_{1r}(\eta), \tag{59}$$
$$A_2=\frac{(1-\xi^2)\eta_1}{(\eta_1+\mu)},\quad l_3=\frac{1}{3\pi^4(k+r)^2}8l_2.$$

Note that $\gamma\approx 0.5$ denotes Euler's constant for the Bessel function of the first kind of order first.

By using the MATHEMATICA program and the boundary conditions given in equations (42) and (52), we have the constants $c_1, c_2, \ldots, c_{12}$.

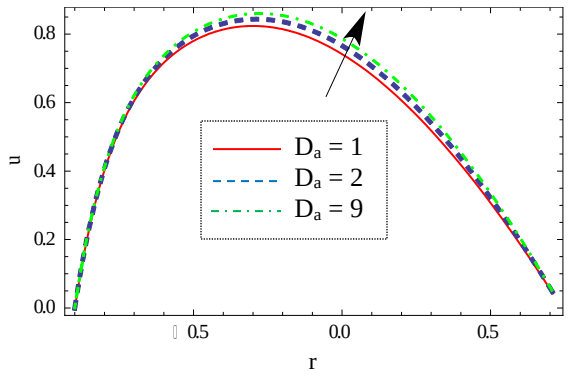

Fig. 2a. variation of D_a on u when E_1= 0.05; E_2= 0.04; E_3= 0.01; ϵ = 0.2; k=1.5; x = -0.2; t = 0.1; $\eta_1 = 0.1$; μ = 0.1; ξ = 1.5; W_e = 0.1; γ = 0.5.

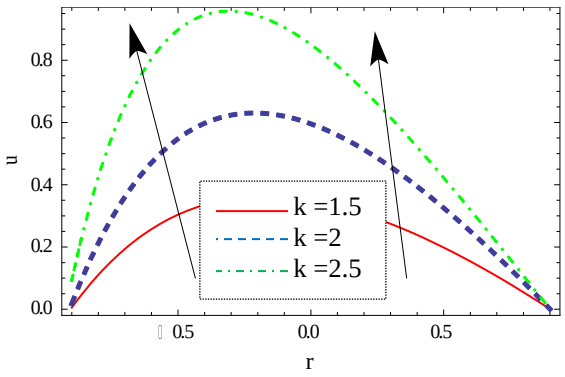

Fig. 2b. variation of k on u when E_1= 0.05; E_2= 0.03; E_3= 0.01; ϵ = 0.1; D_a =1; x = -0.2; t = 0.1; $\eta_1 = 0.1$; μ = 0.1; ξ = 1.3; W_e = 0.1; γ = 0.5.

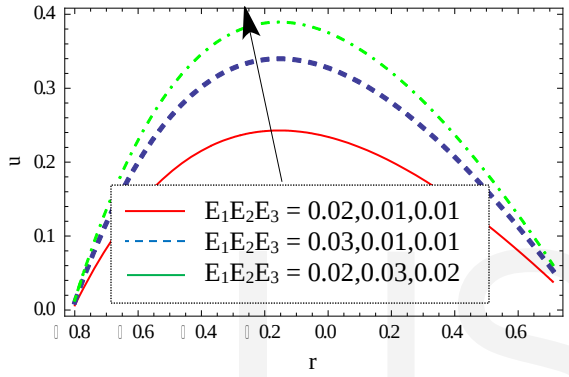

Fig. 2c. variation of compliant wall parameters on u when ϵ = 0.2; k=1.5; x = -0.2; t = 0.1; $\eta_1 = 0.1$; μ = 0.1; M = 1; D_a = 1; ξ = 1.5; W_e = 0.1; γ = 0.5.

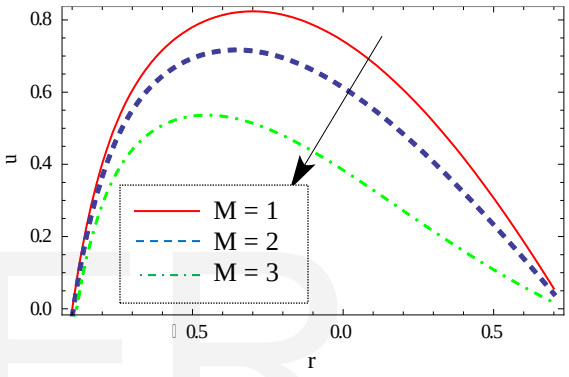

Fig. 2d. variation of M on u when E_1= 0.05; E_2= 0.04; E_3= 0.01; ϵ = 0.2; D_a =1; x = -0.2; t = 0.1; $\eta_1 = 0.1$; μ = 0.1; ξ = 1.5; k= 1.5; W_e = 0.1; γ = 0.5.

4. Results and discussion

Our interest in this section is to study the variation of various parameters on the axial velocity $u = u_0 + W_e^2 u_1 = -\psi_{0r} - W_e^2 \psi_{1r}$, stream function ψ, temperature θ, concentration ϕ and heat transfer coefficient Z. In particular, the effects of compliant wall parameters (E_1,E_2 and E_3), Brinkman number B_r , Schimdt number S_c , curvature parameters k , Weissenberg number W_e , Hartman number M , Darcy number D_a and slip parameter ξ have been disclosed.

Fig.2 shows the behavior of parameters involved in the axial velocity u. Fig.2a indicates that the axial velocity increases by increasing D_a. This Fig. also shows for small curvature and the axial velocity is not symmetric about the centre line of the channel. Fig.2b describes the behavior of curvature parameter k on the velocity. It is found that velocity increases near the lower wall of the channel when there is an increase in the curvature parameter k. Fig.2c describes the behavior of compliant wall parameters (E_1,E_2 and E_3) on the velocity. It is found that velocity decreases with an increase in E_3 . The axial velocity is increasing function of E_1 and E_2. The variation of Hartman number M on u is shown in Fig.2d. We notice that velocity profile is not symmetric about the central line of the channel due to curvature and we notice that axial velocity decreases with an increase in M.

Fig.3 indicates the behavior of parameters appearing in the temperature distribution. Fig.3a shows that the magnitude of temperature increases as W_e increases.It is further noticed.

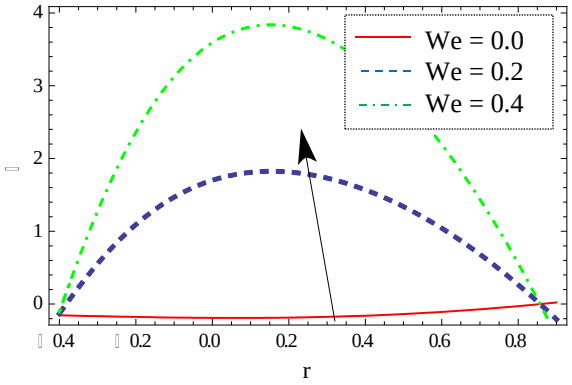

Fig. 3a. variation of W_e on θ when E_1= 0.4; E_2= 0.04; E_3= 0.1; ϵ = 0.15; k=1.5; x = -0.2; t = 0.1; $\eta_1 = 0.6$; μ = 0.5; M = 1; D_a = 1; ξ = 1.9; B_r = 0.5; γ = 0.5.

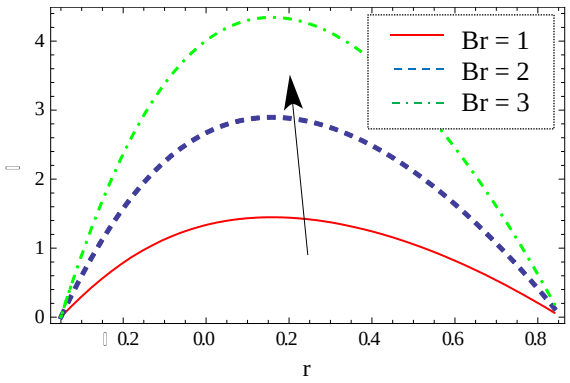

Fig. 3b. variation of B_r on θ when E_1= 0.4; E_2= 0.03; E_3= 0.1; ϵ = 0.15; k=1.5; x = -0.2; t = 0.1; $\eta_1 = 0.8$; M =1; D_a =1; μ = 0.6; ξ = 1.9; W_e = 0.1; γ = 0.5.

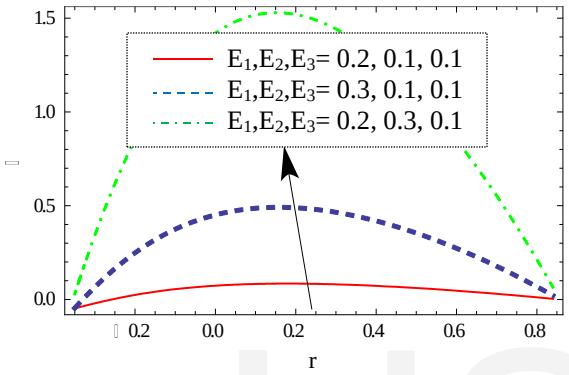

Fig. 3c. variation of compliant wall parameters on θ when ϵ = 0.15; k=1.5; x = -0.2; t = 0.1; $\eta_1 = 0.8$; μ = 0.5; M = 1; D_a = 1; ξ = 1.9; B_r = 0.5; W_e = 0.1; γ = 0.5.

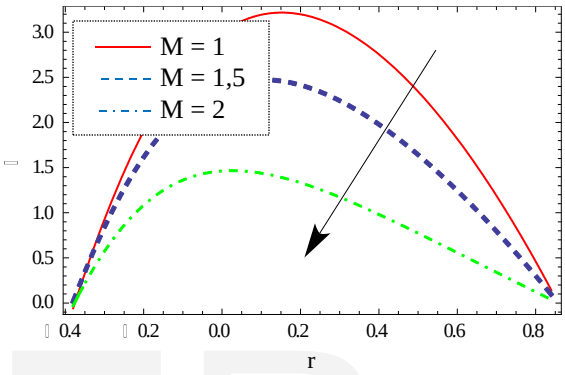

Fig. 3d. variation of M on θ when E_1= 0.5; E_2= 0.04; E_3= 0.01; ϵ = 0.15; D_a =1; x = -0.2; t = 0.1; $\eta_1 = 0.8$; μ = 0.6; ξ = 1.9; k= 1.5; B_r = 0.5; W_e = 0.1; γ = 0.5.

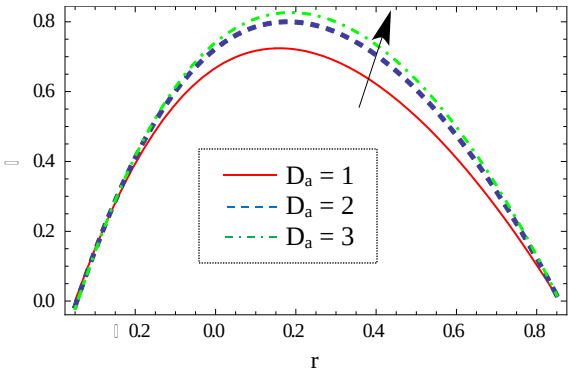

Fig. 3e. variation of D_a on θ when E_1= 0.4; E_2= 0.03; E_3= 0.1; ϵ = 0.15; k=1.5; x = -0.2; t = 0.1; $\eta_1 = 0.8$; μ = 0.6; ξ = 1.9; M =1; B_r = 0.5; W_e = 0.1; γ = 0.5.

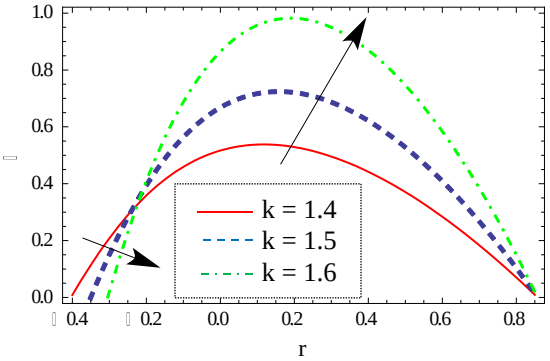

Fig. 3f. variation of k on θ when E_1= 0.4; E_2= 0.03; E_3= 0.1; ϵ = 0.15; D_a=1; x = -0.2; t = 0.1; $\eta_1 = 0.8$; μ = 0.6; ξ = 1.9; M =1; B_r = 0.5; W_e = 0.1; γ = 0.5.

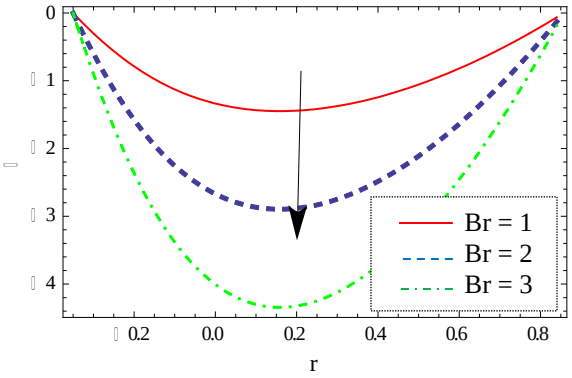

Fig. 4a. variation of B_r on ϕ when E_1= 0.4; E_2= 0.03; E_3= 0.1; ϵ = 0.15; k=1.5; x = -0.2; t = 0.1; $\eta_1 = 0.8$; M =1; D_a =1; μ = 0.6; ξ = 1.9; W_e = 0.1; S_c = 1; S_r = 1; γ = 0.5.

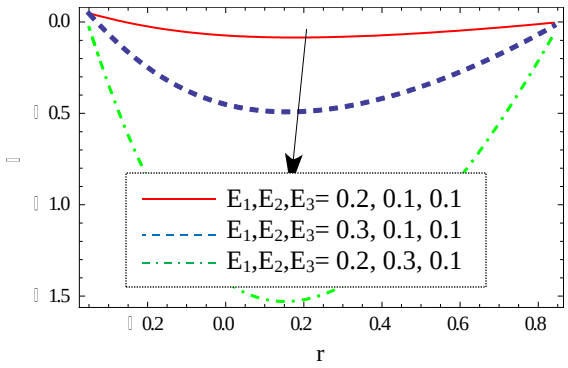

Fig. 4b. variation of compliant wall parameters on ϕ when ϵ = 0.15; k=1.5; x = -0.2; t = 0.1; $\eta_1 = 0.8$; μ = 0.5; M = 1; D_a = 1; ξ = 1.9; B_r = 0.5; W_e = 0.1 S_c = 1; S_r = 1;; γ = 0.5.

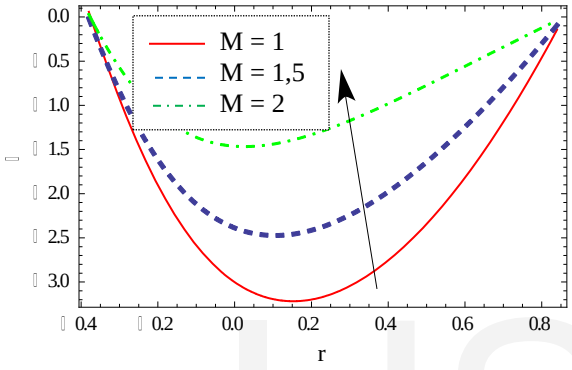

Fig. 4c. variation of M on ϕ when E_1= 0.5; E_2= 0.04; E_3= 0.01; ϵ = 0.15; D_a =1; x = -0.2; t = 0.1; $\eta_1 = 0.8$; μ = 0.6; ξ = 1.9; k= 1.5; B_r = 0.5; W_e = 0.1; S_c = 1; S_r = 1; γ = 0.5.

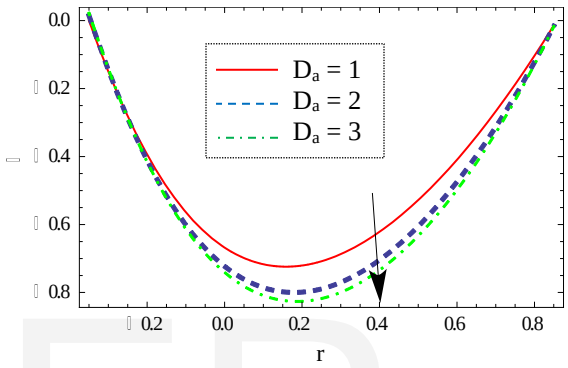

Fig. 4d. variation of D_a on ϕ when E_1= 0.4; E_2= 0.03; E_3= 0.1; ϵ = 0.15; k=1.5; x = -0.2; t = 0.1; $\eta_1 = 0.8$; μ = 0.6; ξ = 1.9; M =1; B_r = 0.5; W_e = 0.1; S_c = 1; S_r = 1; γ = 0.5.

Fig.3b illustrates that the temperature increases when Brinkman number increases. It is shown in Fig.3c that temperature increases with an increase of E_1 and E_2 and decreases with the increase of E_3 . Fig.3d discusses the behavior of Hartman number M which shows that temperature decreases with an increase in M. Fig.3e depicts that θ increases as the tilt of the temperature profile is towards right. Fig.3f depicts that temperature decreases near the lower wall of the channel and increases in the other part of the channel when curvature parameter increases.

Fig.4 represents the behavior of various parameters on the concentration distribution. It is observed from Fig.4a that the concentration decreases as B_r increases. Fig.4b shows that concentration distribution increases with an increase of E_1,E_2 and E_3 in curved channel. Fig.4c illustrates that concentration increases when there is an increase in Hartman number M. Fig.4d discusses the behavior of Darcy number D_a which shows that concentration decreases with an increase in D_a . Fig.4e shows that concentration distribution decreases near the upper wall of the channel with an increase in k. Fig.4f illustrates that concentration decreases when there is an increase in Schmidt number S_c.

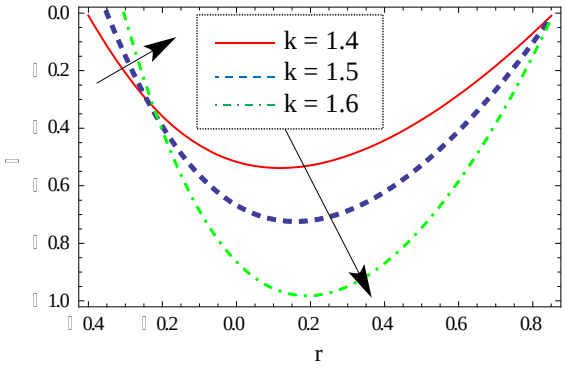

Fig. 4e. variation of k on ϕ when E_1= 0.4; E_2= 0.03; E_3= 0.1; ϵ = 0.15; D_a=1; x = -0.2; t = 0.1; $\eta_1 = 0.8$; μ = 0.6; ξ = 1.9; M =1; B_r = 0.5; W_e = 0.1; S_c = 1; S_r = 1; γ = 0.5.

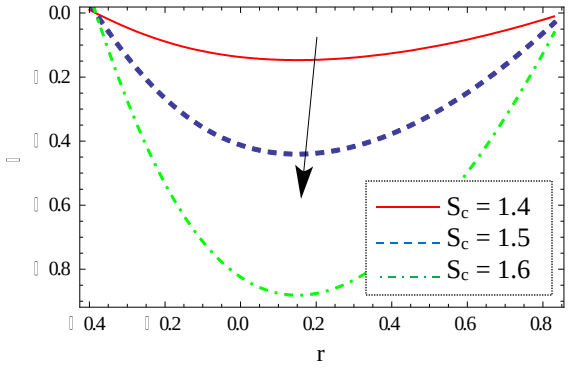

Fig. 4f. variation of S_c on ϕ when E_1= 0.4; E_2= 0.03; E_3= 0.1; ϵ = 0.15; D_a=1; k = 1.5; x = -0.2; t = 0.1; $\eta_1 = 0.8$; μ = 0.6; ξ = 1.9; M =1; B_r = 0.5; W_e = 0.1; S_r = 1; γ = 0.5.

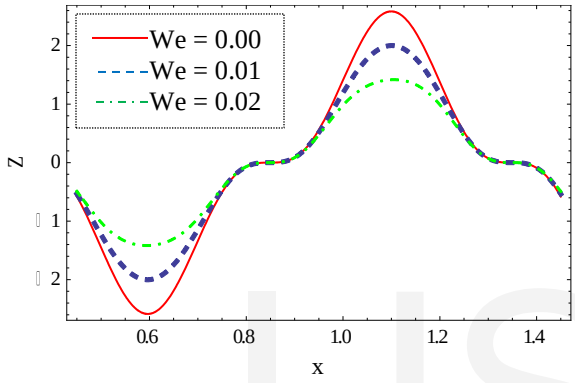

Fig. 5a. variation of W_e on Z when E_1= 0.05; E_2= 0.04; E_3= 0.01; ϵ = 0.15; D_a=1; ; k = 1.5 x = -0.2; t = 0.1; $\eta_1 = 0.6$; μ = 0.5; ξ = 1.8; M =1; B_r = 0.5; γ = 0.5.

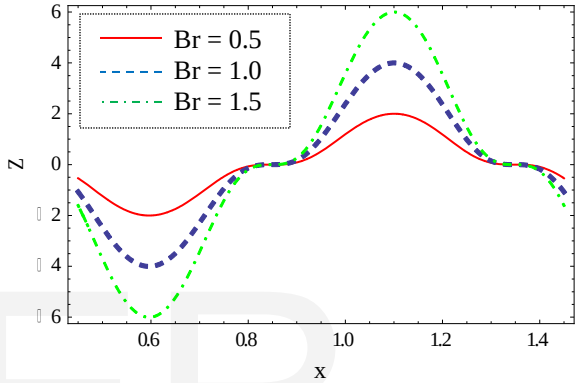

Fig. 5b. variation of B_r on Z when E_1= 0.05; E_2= 0.04; E_3= 0.01; ϵ = 0.15; D_a=1; k = 1.5; x = -0.2; t = 0.1; $\eta_1 = 0.6$; μ = 0.5; ξ = 1.8; M =1; W_e = 0.01; γ = 0.5.

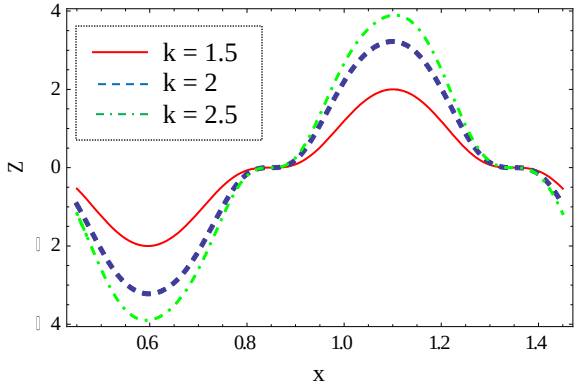

Fig. 5c. variation of k on Z when E_1= 0.05; E_2= 0.04; E_3= 0.01; ϵ = 0.15; D_a=1; x = -0.2; t = 0.1; $\eta_1 = 0.6$; μ = 0.5; ξ = 1.8; M =1; B_r = 0.5; W_e = 0.01; γ = 0.5.

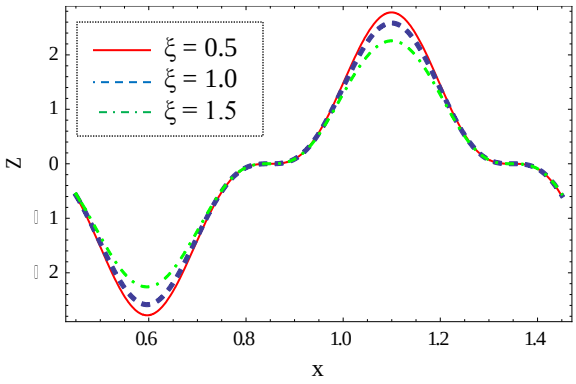

Fig. 5d. variation of ξ on Z when E_1= 0.05; E_2= 0.04; E_3= 0.01; ϵ = 0.15; D_a=1; x = -0.2; t = 0.1; $\eta_1 = 0.6$; μ = 0.5; M =1; B_r = 0.5; W_e = 0.01; γ = 0.5.

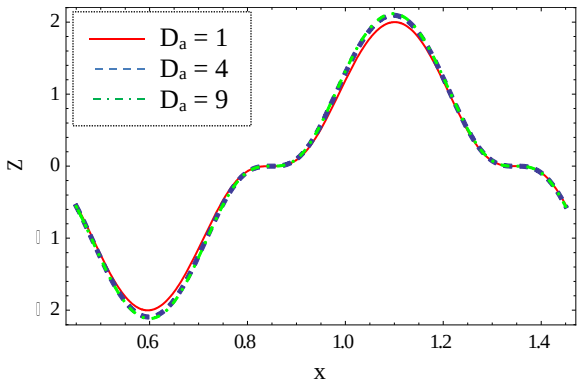

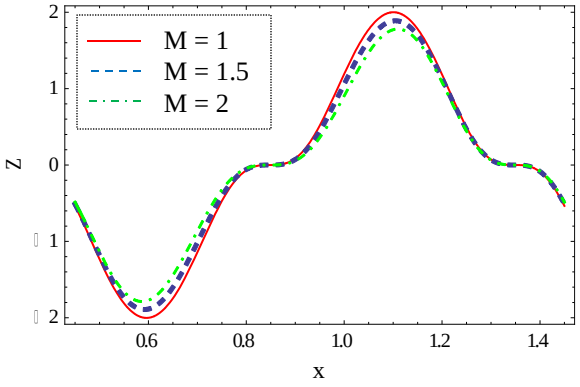

Fig. 5e. variation of D_a on Z when E_1= 0.05; E_2= 0.04; E_3= 0.01; ϵ = 0.15; k =1.5; x = -0.2; t = 0.1; η_1 = 0.6; μ = 0.5; ξ = 1.8; M =1; B_r = 0.5; W_e = 0.01; γ = 0.5.

Fig. 5f. variation of M on Z when E_1= 0.05; E_2= 0.04; E_3= 0.01; ϵ = 0.15; D_a = 1; k =1.5; x = -0.2; t = 0.1; η_1 = 0.6; μ = 0.5; ξ = 1.8; B_r = 0.5; W_e = 0.01; γ = 0.5.

Fig.5 presents the behavior of involved parameters in heat transfer coefficient Z. Fig.5a shows that the absolute value of heat transfer coefficient decreases when W_e increases. Fig.5b depicts that Z increases by increasing B_r. Fig.5c shows that the heat transfer coefficient increases with an increas in curvature parameter. Fig.5d depicts that the heat transfer coefficient decreases with an increase in slip parameter. Fig.5e shows that the heat transfer coefficient increases with an increase in Darcy number. Fig.5f depicts that the heat transfer coefficient decreases with an increase in Hartman number.

Fig.6 indicates the behavior of parameters in the stream function. Fig.6a and b show that the bolus increases with an increase in W_e . Fig.7a and b are plotted to study the behavior of curvature parameter. This Fig. shows that the size of bolus decreases when M increases. Fig.8a and b illustrates that the bolus increases with an increase in D_a.

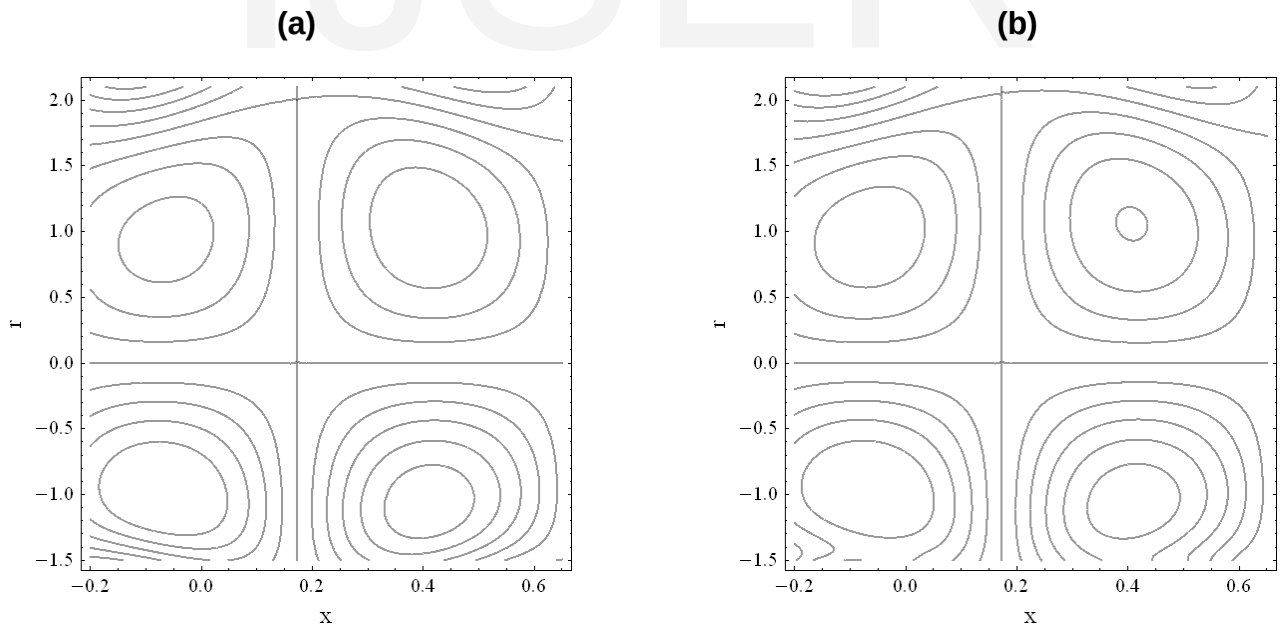

Fig.6. Variation of W_e on ψ when E_1= 0.02; E_2= 0.01; E_3= 0.1; ϵ = 0.1; t = 0; ξ = 0.1; η_1= 0.1; μ = 0.1; k = 1.7; M = 1; D_a = 1; γ = 0.5; **(a):** W_e = 0.00; **(b):** W_e = 0.04.

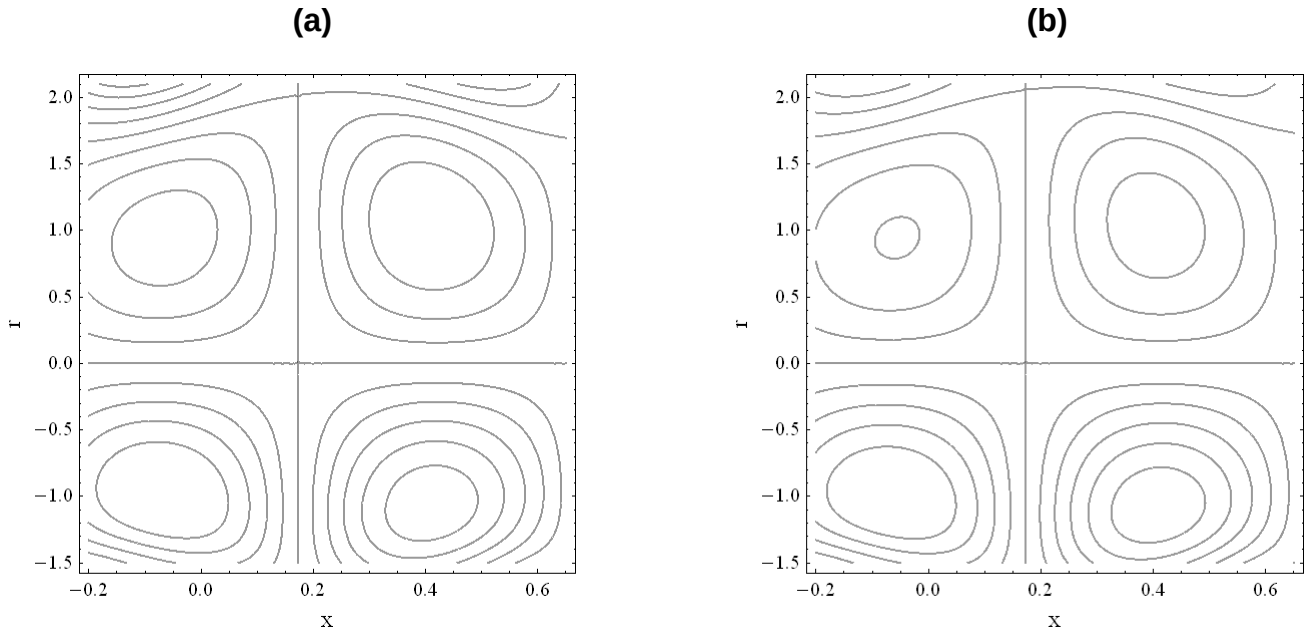

Fig.7. Variation of M on ψ when E_1= 0.02; E_2= 0.01; E_3= 0.1; ϵ = 0.1; t = 0; ξ = 0.1; η_1= 0.1; μ = 0.1; k = 1.7; W_e=0.01; D_a = 1; γ = 0.5; **(a):** M = 0 ; **(b):** M = 1.

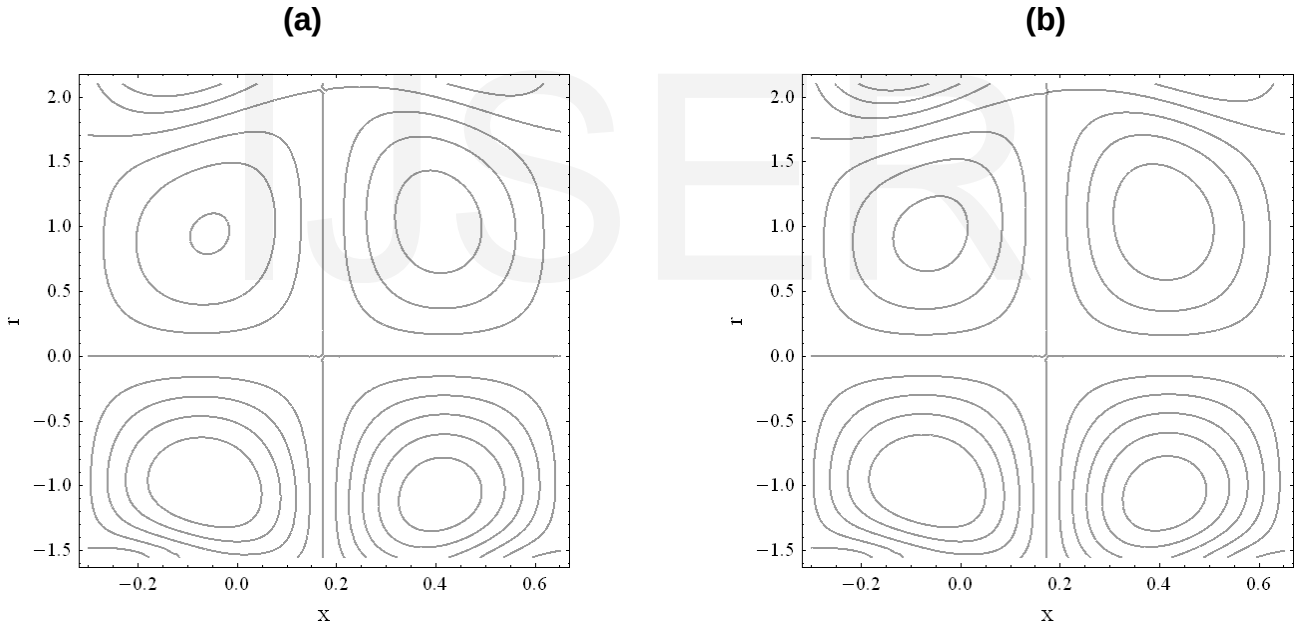

Fig.8. Variation of D_a on ψ when E_1= 0.02; E_2= 0.01; E_3= 0.1; ϵ = 0.1; t = 0; ξ = 0.1; η_1= 0.1; μ = 0.1; k = 1.7;W_e=0.01; M = 1; γ = 0.5; **(a):** D_a = 1 ; **(b):** D_a = 2.

5. Concluding remarks

In this study the effects of heat and mass transfer and induced magnetic field on the peristaltic transport of the Johnson-Segalman fluid in a porous curved channel are discussed. Coupled equations are solved by employing perturbation method. The following observation have been found:

- Not symmetry in the profiles of u, θ, ϕ and Z disturbed because of curvature effects.
- The magnitude of velocity u and temperature θ increasing functions of k and D_a while it decreases when M increases.

- The axial velocity in J-S fluid is larger than the Newtonian fluid. Due to curvature the velocity profile is tilted towards left whereas temperature and concentration profiles tilted towards right.
- The bolous size in Johnson-Segalman fluid is greater than the viscous fluid.
- The parameters appearing in the temperature distribution have opposite effect on the concentration distribution.

References

[1] Latham, T. W. Fluid Motion in a Peristaltic Pump, M. S. dissertation, Massachusetts Insitute of Technology, Cambridge **(1966)** .

[2] Jaffrin, M. Y. and Shapiro, A. H. Peristaltic pumping. Annual Review of Fluid Mechanics, 3, 13–16 **(1971)**.

[3] Radhakrishnamacharya, G. and Murty, V. R. Heat transfer to peristaltic transport in a nonuniform channel. Defence Science Journal, 43(3), 275–280 **(1993)**.

[4] Vajravelu, K., Radhakrishnamacharya, G., and Murty, V. R. Peristaltic flow and heat transfer in a vertical porous annulus, with long wave approximation. International Journal of Non-Linear Mechanics, 42(5), 754–759 **(2007)**.

[5] Srinivas, S. and Kothandapani, M. Peristaltic transport in an asymmetric channel with heat transfer—a note. International Communications in Heat and Mass Transfer, 35(4), 514–522 **(2008)**.

[6] Mekheimer, K. S. and Elmaboud, Y. A. The influence of heat transfer and magnetic field on peristaltic transport of a Newtonian fluid in a vertical annulus: application of an endoscope. Physics Letters A, 372(10), 1657–1665 **(2008)**.

[7] Srinivas, S., Gayathri, R., and Kothandapani, M. Mixed convective heat and mass transfer in an asymmetric channel with peristalsis. Communications in Nonlinear Science and Numerical Simulation, 16(4), 1845–1862 **(2011)**.

[8] Srinivas, S. and Muthuraj, R. Effects of chemical reaction and space porosity on MHD mixed convective flow in a vertical asymmetric channel with peristalsis. Mathematical and Computer Modelling, 54(5-6), 1213–1227 **(2011)**.

[9] Nadeem, S. and Akbar, N. S. Influence of radially varying MHD on the peristaltic flow in an annulus with heat and mass transfer. Journal of the Taiwan Institute of Chemical Engineers, 41(3), 286–294 **(2010)**.

[10] Elmaboud, Y. A. Influence of induced magnetic field on peristaltic flow in an annulus. Communications in Nonlinear Science and Numerical Simulation, 17(2), 685–698 **(2012)**.

[11] Tripathi, D., Panday, S. K., and Das, S. Peristaltic transport of a generalized Burgers' fluid application to the movement of chyme in small intestine. Acta Astronautica, 69(1-2), 30–38 **(2011)**.

[12] Tripathi, D. A mathematical model for the peristaltic flow of chyme movement in small intestine. Mathematical Biosciences, 233(2), 90–97 **(2011)**.

[13] T. Hayat, Y. Wang, A.M. Siddique, K. Hutter, Peristaltic motion of Johnson Segalman fluid in a planar channel, Math. Prob. Eng. 2003, 1–23 **(2003)**.

[14] M. Elshahed, M.H. Haroun, Peristaltic transport of Johnson–Segalman fluidunder effect of a magnetic field, Math. Prob. Eng. 2005, 663–677 **(2005)**.

[15] T. Hayat, A. Afsar, N. Ali, Peristaltic transport of a Johnson–Segalman fluid in an asymmetric channel, Math. Comput. Mod. 47, 380–400 **(2005)**.

[16] Y. Wang, T. Hayat, K. Hutter, Peristaltic transport of a Johnson–Segalman fluidthrough a deformable tube, Theor. Comput. Fluid Dyn. 21, 369–380 **(2007)**.

[17] S. Nadeem, N.S. Akbar, Influence of heat and mass transfer on the peristaltic flow of a Johnson–Segalman fluid in a vertical asymmetric channel with induced MHD, J. Taiwan Inst. Chem. Eng. 42, 58–66 **(2011)**.

[18] N. Ali, M. Sajid and T. Hayat, Long wavelength flow analysis in a curved channel, Zeitschrift Fur Naturforschung A 65, 191–196 **(2010)**.

[19] N. Ali, M. Sajid, T. Javed and Z. Abbas, Heat transfer analysis of peristaltic flow in a curved channel, Int J Heat Mass Transfer 53, 3319–3325 **(2010)**.

[20] N. Ali, M. Sajid, T. Javed and Z. Abbas, Non-Newtonian flow induced by a peristaltic waves in a curved channel, European J Mech B/Fluids 29, 387–394 **(2010)** .

[21] Ebaid A, Khaled SM, An exact solution for the boundary value problem with application in fluid mechanics and comparison with the regular perturbation solution. Abst Appl Anal, Article ID 172590 **(2014)**.

IJSER